



Published in final edited form as:

*Epilepsia*. 2018 February ; 59(2): 333–344. doi:10.1111/epi.13990.

## Neonatal phenobarbital exposure disrupts GABAergic synaptic maturation in rat CA1 neurons.

Nour Al Muhtasib<sup>#1</sup>, Alberto Sepulveda-Rodriguez<sup>#1,2</sup>, Stefano Vicini<sup>1,2,3</sup>, and Patrick A. Forcelli<sup>1,2,3</sup>

<sup>1</sup>Department of Pharmacology and Physiology

<sup>2</sup>Interdisciplinary Program in Neuroscience

<sup>3</sup>Department of Neuroscience, Georgetown University, Washington DC

# These authors contributed equally to this work.

### Summary:

**Objective:** Phenobarbital is the most commonly utilized drug for the treatment of neonatal seizures. The use of phenobarbital continues despite growing evidence that it exerts suboptimal seizure control and is associated with long-term alterations in brain structure, function, and behavior. Alterations following neonatal phenobarbital exposure include acute induction of neuronal apoptosis, disruption of synaptic development in the striatum, and a host of behavioral deficits. These behavioral deficits include those in learning and memory mediated by the hippocampus. However, the synaptic changes caused by acute exposure to phenobarbital that lead to lasting effects on brain function and behavior remain understudied.

**Methods:** Postnatal day (P)7 rat pups were treated with phenobarbital (75 mg/kg) or saline. On P13–14 or P29–37, acute slices were prepared and whole-cell patch clamp recordings were made from CA1 pyramidal neurons.

**Results:** At P14 we found an increase in miniature inhibitory post-synaptic current (mIPSC) frequency in the phenobarbital-exposed as compared to the saline-exposed group. In addition to this change in mIPSC frequency, the phenobarbital group displayed larger bicuculline-sensitive tonic currents, decreased capacitance and membrane time constant, and a surprising persistence of giant depolarizing potentials. At P29+, the frequency of mIPSCs in the saline-exposed group had increased significantly from the frequency at P14, typical of normal synaptic development; at this age the phenobarbital-exposed group displayed a lower mIPSC frequency than did the control group. sIPSC amplitude was unaffected at either P14 or P29+

---

**Correspondence:** Dr. Patrick A. Forcelli, Dept of Pharmacology & Physiology, Georgetown University, 3970 Reservoir Road NW NRB W209B, Washington DC 20007, paf22@georgetown.edu, Office: 202-687-5194.

Author Contributions:

Designed Study: PAF

Performed Experiments: NA, AS, SV, PAF

Analyzed Data: NA, AS, SV, PAF

Wrote Manuscript: NA, AS, SV, PAF

**Disclosure.** No authors report conflicts of interest. We confirm that we have read the Journal's position on issues involved in ethical publication and affirm that this report is consistent with those guidelines.

## Keywords

patch-clamp; cell death; neonatal; gestational; teratogen; apoptosis

---

## 1. Introduction

The treatment of epilepsy in early life is complicated by the fact that therapeutic interventions can adversely impact brain maturation. The exquisite sensitivity of the developing brain to perturbations in the balance of excitation and inhibition can result in even transient alterations producing long-lasting effects. This balance is the target of many anti-seizure medications, including phenobarbital, the most commonly utilized drug for the treatment of neonatal seizures.<sup>1</sup> The use of phenobarbital continues in neonatal neurology despite compelling evidence that (1) it provides insufficient seizure control,<sup>2</sup> and (2) it is associated with long-term alterations in cognitive function.<sup>3</sup>

In an effort to understand the impact of phenobarbital, and other anti-seizure medications, on brain development, preclinical screening models have been employed. Treatment of rodents during the “brain growth spurt” occurring in the first postnatal week is thought to mirror a period spanning the third trimester of gestation through early infancy in humans.<sup>4</sup> Exposure to phenobarbital during this confined neonatal period produces a variety of sequelae.

First, phenobarbital, as well as therapeutically relevant doses of phenytoin, clonazepam, diazepam, vigabatrin, retigabine, and sodium valproate, produce a profound increase in the magnitude of developmental apoptosis.<sup>5–8</sup> While pruning of neurons is a normal part of postnatal brain development, the increased apoptosis caused by these drugs exceeds that seen in normal brain development by as much as 10-fold. Similar effects have been reported following postnatal exposure to ethanol<sup>9</sup> and anesthetic agents<sup>10</sup>. Enhanced apoptosis has been described both in the developing grey and white matter, with regions such as the striatum, thalamus, and hippocampus showing particularly high degrees of cell death. However, the amount of cell loss observed is likely insufficient to account for long term neurobehavioral changes.

Second, phenobarbital, as well as phenytoin and lamotrigine, induce a profound impairment in striatal synaptic development.<sup>11,12</sup> Strikingly, a single exposure to phenobarbital on postnatal day (P)7 disrupted the normal increase in the frequency of both inhibitory and excitatory post-synaptic currents in striatal medium spiny neurons.<sup>11</sup> This co-occurred with a persistence of immature structural phenotypes of dendritic spines, with effects far outlasting the initial drug exposure.<sup>11</sup> Consistent with this impaired striatal function, lasting deficits in striatal mediated reversal learning behavior were reported.<sup>11</sup> This alteration in function of neurons that survive the initial pro-apoptotic insult may provide a link between early life drug exposure and later-in-life behavioral changes.

Third, phenobarbital, and several other anti-seizure medications induce long-lasting alterations in behavior.<sup>13–18</sup> Deficits in a variety of hippocampal-mediated behaviors have been reported, including impaired: water maze learning,<sup>14,19</sup> fear conditioning,<sup>14</sup> passive avoidance learning,<sup>15,16</sup> Y maze and radial arm maze performance,<sup>18,20</sup> and sensorimotor

gating.<sup>12–16</sup> However, the impact of neonatal phenobarbital exposure on the synaptic development within the hippocampus has not been previously evaluated.

In order to begin to understand how early life exposure to PB can impact later-in-life behaviors, we examined the synaptic physiology of neurons in CA1 after a single earlier-in-life PB treatment. We examined the frequency, amplitude, and kinetics of spontaneous and miniature inhibitory postsynaptic currents in acute slices through CA1 one week and 3–5 weeks after exposure to phenobarbital. We also examined the impact of phenobarbital treatment on tonic GABA currents and on the presence of giant depolarizing potentials (GDPs), which are large GABAergic currents that serve as an organizing hallmark of hippocampal physiology early in postnatal development.<sup>21</sup>

## Materials and Methods

### Animals

Timed-pregnant Sprague-Dawley rats were obtained from Harlan Laboratories (Indianapolis, IN). Upon arrival at Georgetown University, they were housed on a standard 12 hour:12 hour light:dark cycle with food and water available *ad libitum*. The day of parturition was designated as postnatal day (P) 0. Eight independent litters contributed to this study, with a single pair of animals from each litter (one saline, one phenobarbital) used for each experiment. The procedures in this manuscript were performed with approval of the Georgetown University IACUC.

### Systemic Drug Treatment

Sodium phenobarbital (PB, 75 mg/kg; 5-ethyl-5-phenyl-1,3-diazinane-2,4,6-trione; Sigma, St Louis, MO) was dissolved in normal (0.9%) saline. The drug was injected intraperitoneally at a volume of 0.01 ml/g. This dose of phenobarbital was selected based on prior reports of phenobarbital efficacy in developing animals and falls within the anticonvulsant range in neonatal rats.<sup>22,23</sup> This dose was also selected based on its ability to induce neuronal apoptosis<sup>5</sup> and impair striatal synaptic maturation.<sup>11</sup>

On P7, animals were briefly removed from their dam, weighed and treated. Following treatment, pups were maintained with their dam until P13–P14, at which time they were used for electrophysiological experiments; eight pups of each treatment were used for these experiments. For adult recordings, pups were weaned at P21–23 and pair housed until the day of the experiment (P29–35).

### Brain slice preparation

Horizontal slices (275  $\mu$ m thick) through the hippocampus were prepared from postnatal day 13–14 (P13–14, juvenile) or P29–35 (young adult) male and female rats. Rats were anesthetized with isoflurane and killed by decapitation in agreement with the guidelines of the American Veterinary Medical Association Panel on Euthanasia. All animal procedures were performed in accordance with Georgetown University's animal care committee's regulations.

For the juvenile animals, the whole brain was removed and placed in an ice-cold cutting solution containing (in mM): NaCl (87.3), KCl (2.7), CaCl<sub>2</sub> (0.5), MgSO<sub>4</sub> (non-hydrate) (6.6), NaH<sub>2</sub>PO<sub>4</sub> (1.4), NaHCO<sub>3</sub> (26.0), glucose (25.0), sucrose (75.1) (all from Sigma, St. Louis, MO, USA). A Vibratome 3000 Plus Sectioning System (Vibratome, St. Louis, MO, USA) was used to prepare slices. The slices were incubated in artificial cerebrospinal fluid (aCSF) containing (in mM): NaCl (123.9), KCl (4.5), Na<sub>2</sub>HPO<sub>4</sub> (1.2), NaHCO<sub>3</sub> (26.0), CaCl<sub>2</sub> (2.0), MgCl<sub>2</sub> (1.0), and glucose (10.0) at 305 mOsm at 32 °C for 30 minutes. The slices were then incubated for an additional 30 minutes in the same solution at room temperature. All solutions were continuously bubbled with 95% O<sub>2</sub>/5% CO<sub>2</sub> to maintain a pH of 7.4.

Adult female and male rats were anesthetized with isoflurane and perfused using a protective recovery solution<sup>24</sup> containing (mM): N-methyl-D-glucamine (93), KCl (2.5), NaH<sub>2</sub>PO<sub>4</sub> (1.2), NaHCO<sub>3</sub> (30.0), HEPES (20.0), glucose (25.0), ascorbic acid (5.0), thiourea (2.0), sodium pyruvate (3.0), N-acetyl-L-cysteine (5.0), MgSO<sub>4</sub> (10.0), and CaCl<sub>2</sub> (0.5) at 305 mOsm and pH 7.4. As with the young animals, the rats were decapitated and the whole brain was removed and placed in ice cold recovery solution. The Vibratome was used to prepare 275 μm hippocampal horizontal slices. The slices were incubated for 10 minutes in the recovery solution at 32 °C before transfer to a room temperature incubation solution containing NaCl (92.0), KCl (2.5), NaH<sub>2</sub>PO<sub>4</sub> (1.2), NaHCO<sub>3</sub> (30.0), HEPES (20.0), glucose (25.0), ascorbic acid (5.0), thiourea (2.0), sodium pyruvate (3.0), N-acetyl-L-cysteine (5), MgSO<sub>4</sub> (2), and CaCl<sub>2</sub> (2) at 305 mOsm and pH 7.4. After an hour-long incubation, electrophysiology recordings were performed in aCSF as described with the young rats.

## Recording

Slices were visualized using an upright microscope (E600FN, Nikon, Tokyo, Japan) equipped with Nomarski optics and a 60X water immersion objective with a long working distance (2 mm) and high numerical aperture (1.0). Recording electrodes with a resistance of 4–6 MΩ were prepared from borosilicate glass capillaries (Wiretrol II; Drummond, Broomall, PA, USA).

A KCl-based internal solution containing (in mM): KCl (145), HEPES (10), ATP-Mg (5), GTP-Na (0.2), EGTA (10) and adjusted to pH 7.2 with KOH was used for all recordings. Voltage-clamp recordings were achieved using the whole-cell configuration method at a holding voltage of –60 mV using the MultiClamp 700B amplifier (Molecular Devices, Sunnyvale, CA, USA).

All recordings were performed at room temperature, 22–24 °C. Recordings were performed from pyramidal cells in the CA1 region of the hippocampus. The firing pattern in response to hyperpolarizing and depolarizing current injections was obtained. Access resistance was monitored periodically during the experiment and recordings with a >20% change were discarded. Recordings were filtered at 2 kHz with a low-pass Bessel filter and digitized at 20 kHz using a personal computer equipped with Digidata 1440A data acquisition board and pCLAMP10 software (both from Molecular Devices).

Stock solutions of bicuculline methobromide (BMR) and tetrodotoxin (TTX; both from Sigma) were prepared in water. Working solutions were prepared in aCSF and applied to the slice via Y tube (Murase).

### Data analysis

Data analysis was performed using Clampfit 10 software (Molecular Devices). Spontaneous inhibitory postsynaptic currents (sIPSCs) and miniature inhibitory postsynaptic currents (mIPSCs) were detected using template search in the Clampfit 10 software and were visually confirmed. All detected events were used to calculate IPSC frequency; however, for amplitude and decay kinetics, superimposing events were excluded. Decay kinetics were measured using double exponential fitting as previously described.<sup>25</sup>

NBQX was not included during IPSC measurements to avoid perturbing the network activity. However, AMPA-mediated spontaneous EPSCs could easily be identified by the rapid decay kinetics and were thus excluded from the IPSC analysis as previously described. <sup>11</sup> mIPSCs were isolated by application of TTX (0.5  $\mu$ M), with an average of 60 events per cell used for frequency analysis. BMR-sensitive tonic GABA currents were revealed by application of BMR (25  $\mu$ M) on the background of TTX, and the shift in baseline holding current was measured from the peak histogram of the current trace in the period immediately preceding (10 s) and after (10 s) BMR application. During application of BMR, IPSCs were abolished. During PSC detection, GDPs were excluded from measurements of frequency, decay, and amplitude.

Resistance and capacitance were measured at a resting membrane potential of  $-60$  mV from the voltage response to  $-10$  pA hyperpolarizing currents. Current-Voltage (IV) relation analysis was performed by manual counting of action potentials at each depolarizing current step. This was performed by two independent evaluators. Similarly, the presence of giant depolarizing potentials (GDPs) were evaluated by two observers; only events  $>10$ mV in amplitude were included; In cases where spikes were present on top of a GDP, the amplitude was measured from the preceding baseline to the peak between spikes. GDPs were also distinguished from unitary IPSCs based on their longer duration and greater amplitude. Data analysis was performed while blinded to the treatment status of the animal.

### Statistical Analysis

Data were analyzed using GraphPad Prism (Version 7.0c, GraphPad Software, La Jolla, CA). Prior to analysis, all data were subjected to normality testing (D'Agostino and Pearson's test or Kolmogorov-Smirnov's test). Current (sIPSC, mIPSC, tonic) analyses and intrinsic membrane properties were then analyzed by two-way analysis of variance (ANOVA) with age and treatment as between subject factors. For the proportion of cells displaying GDPs, Fisher's exact test was used. Finally, for current-voltage relationship analyses a repeated measures ANOVA was used (treatment as a between subject factor, stimulus intensity as a repeated measure). For pairwise comparisons (Holm-Sidak corrected), we tested only the comparisons for which we had *a priori* hypotheses (drug treatment as a function of age, and drug treatment within age). Two-tailed tests were used for all comparisons aside from current frequency, where we had a clear *a priori* directional

hypothesis (i.e., the frequency of IPSCs increases with age). P values < 0.05 were considered to be statistically significant.

Figures display box-and-whisker plots (minimum to maximum) or histograms (mean + standard error of the mean). Values in the text report mean  $\pm$  standard deviation.

## Results

As shown in Figure 1, at both ages examined, cells from control animals and those from animals treated with PB displayed equivalent excitability in current injection protocols conducted in current clamp mode. Increasing amplitude of depolarizing current steps was associated with a significant increase in the number of action potentials fired ( $F_{2,48,96.8}=96.8$ ,  $P<0.0001$ ), however, there was neither a main effect of drug treatment ( $F_{1,39}=0.007$ ,  $P=0.94$ ), a main effect of age ( $F_{1,39}=0.208$ ,  $P=0.65$ ), nor any significant interactions between these variables ( $P_s>0.70$ ). Example traces from cells from a saline-treated [light blue] and phenobarbital treated [dark blue] animal at P14 are shown in Figure 1A and summary data are presented in Figure 1B.

We examined passive membrane properties of CA1 neurons from animals treated with saline or phenobarbital. While not reaching the level of statistical significance, there was a trend toward an increase in input resistance (Fig 1C) as a function of age ( $F_{1,39}=0.3.1$ ,  $P=0.08$ ), but neither a main effect of treatment ( $F_{1,39}=0.21$ ,  $P=0.65$ ), nor a treatment-by-age interaction ( $F_{1,39}=0.099$ ,  $P=0.76$ ). The input resistance of these cells did not differ between treatment groups (Figure 1C, saline, P14 =  $201 \pm 81$  M $\Omega$ ; P29+ =  $261 \pm 82$  M $\Omega$ ; phenobarbital, P14 =  $223 \pm 74$  M $\Omega$ ; P29+ =  $265 \pm 121$  M $\Omega$ ).

Analysis of the membrane time constant (Fig 1D) revealed a significant interaction between age and treatment ( $F_{1,37}=5.39$ ,  $P=0.026$ ), but neither a significant main effect of age ( $F_{1,37}=0.82$ ,  $P=0.37$ ) nor treatment ( $F_{1,37}=0.42$ ,  $P=0.52$ ). This interaction was due to the significant difference between phenobarbital ( $9.8 \pm 3.7$  msec) and saline ( $15.6 \pm 6.6$  msec) treated conditions at P14 ( $P<0.05$ ), and a significant increase in time constant in the phenobarbital group between P14 ( $9.8 \pm 3.7$  msec) and P25 ( $16.1 \pm 7.7$ ;  $P<0.05$ ). As with the time constant, capacitance displayed a significant interaction between treatment and age ( $F_{1,37}=9.97$ ,  $P=0.0032$ ), but neither a main effect of treatment ( $F_{1,37}=0.15$ ,  $P=0.70$ ) nor age ( $F_{1,37}=0.57$ ,  $P=0.45$ ). This was driven by a significant difference between phenobarbital (phenobarbital:  $48 \pm 23$  pF) and saline-treated groups (saline:  $84 \pm 34$  pF) at the P14 time point. There was a non-significant trend toward decreased capacitance in the saline-treated group as a function of age (P14 =  $84 \pm 34$  pF; P29+ =  $43.9 \pm 7.6$  pF;  $P=0.058$ ).

To determine if exposure to PB altered spontaneous inhibitory post-synaptic currents (sIPSCs) we measured their frequency and amplitude in: 26 cells from saline treated animals ( $n=5$ ) at P14, 29 cells from phenobarbital treated animals ( $n=5$ ) at P14, 17 cells from saline treated animals ( $n=3$ ) at P29+, and 13 cells from phenobarbital treated animals at P29+ ( $n=3$ ). As shown in the example in Figure 2A and summary data Figure 2B, sIPSC frequency did not differ as a function of treatment ( $F_{1,81}=2.14$ ,  $P=0.15$ ), or age ( $F_{1,81}=1.79$ ,  $P=0.18$ ). Moreover, there was no interaction between age and treatment ( $F_{1,81}=2.66$ ,

P=0.11). The mean ( $\pm$  standard deviation) of sIPSC frequency was  $1.8 \pm 1.3$  and  $2.6 \pm 1.1$  Hz in cells from saline-treated animals at P14 and P29+, respectively. sIPSC frequency was  $1.9 \pm 1.1$  and  $1.8 \pm 0.75$  Hz in cells from phenobarbital-treated animals at P14 and P29+, respectively.

Analysis of sIPSC amplitude (Figure 2C) revealed a significant main effect of treatment ( $F_{1,81}=5.48$ ,  $P=0.022$ ), a significant treatment-by-age interaction ( $F_{1,81}=4.6$ ,  $P=0.04$ ), but no effect of age ( $P=0.10$ ). These effects were driven by a significant increase in sIPSC amplitude in the saline-treated group from P14 to P29+ ( $55.3 \pm 31.6$  vs.  $82.1 \pm 36.2$  pA;  $P<0.05$ ). This developmental increase was absent in phenobarbital-treated animals ( $53.8 \pm 29.2$  vs  $50.3 \pm 26.8$  pA,  $P=0.73$ ). This difference in developmental trajectory led to a significant difference between saline- and phenobarbital- treated groups at P29+ ( $P<0.05$ ).

We next examined the impact of P7 phenobarbital treatment on miniature inhibitory post-synaptic currents (mIPSCs), recorded in the presence of tetrodotoxin ( $0.5 \mu\text{M}$ ), from 22 cells from saline treated animals at P14, 21 cells from phenobarbital treated animals ( $n=5$ ) at P14, 15 cells from saline treated animals at P29+, and 8 cells from phenobarbital treated animals at P29+ (Figure 3). Representative traces are shown in Figure 3A. Analysis of variance revealed a significant age-by-treatment interaction ( $F_{1,62}=11.15$   $P=0.0014$ ), but neither a significant main effect of treatment nor age ( $P_s<0.34$ ). The interaction effect was driven by a significant ( $P<0.05$ ) developmental increase in mIPSC frequency that was evident in saline-treated ( $0.73 \pm 0.37$  Hz vs  $1.3 \pm 0.75$  Hz) but not phenobarbital-treated ( $1.03 \pm 0.46$  Hz vs  $0.72 \pm 0.25$  Hz) groups (Figure 3B). Moreover, saline and phenobarbital-treated groups differed significantly at both P14 and P29+; at P14, the phenobarbital-treated group displayed a higher mIPSC frequency, whereas at P29+ the phenobarbital-treated group displayed a lower mIPSC frequency. As with sIPSC amplitude, we found that mIPSC amplitude increased in the saline, but not phenobarbital-treated conditions between P14 and P29+ (Figure 3C,  $P<0.05$ ). This was evident in the significant age-by-treatment interaction ( $F_{1,62}=4.37$ ,  $P=0.041$ ), neither the main effect of treatment, nor of age reached the level of statistical significance ( $P_s<0.19$ ). mIPSC decay was significantly quickened from P14 to P25, but did not differ across treatments (Figure 3D). This was revealed by a significant main effect of age ( $F_{1,62}=142.9$ ,  $P<0.0001$ ), but neither a main effect of treatment, nor a treatment-by-age interaction ( $P_s<0.47$ ). Both the saline- and phenobarbital- treated groups showed faster decay kinetics at P29+ as compared to P14 (saline:  $36 \pm 6$  ms vs  $20 \pm 2$  ms; phenobarbital:  $35 \pm 6$  ms vs  $18 \pm 2$  ms at P14 and P29+, respectively;  $P_s<0.0001$ ).

We next examined the effect of P7 exposure to phenobarbital on tonic GABA currents. Presence of tonic current was revealed by Y-tube application of the GABA<sub>A</sub> receptor antagonist bicuculline methobromide ( $25 \mu\text{M}$ ) as in the examples from the P14 animals in Figure 4A. As shown in Figure 4B, in cells ( $n=21$ ) from control animals at P14, the mean amplitude of tonic current was  $12 \pm 8$  pA, whereas in cells from animals treated with phenobarbital ( $n=24$ ), the mean amplitude was  $20 \pm 10$  pA. At P29+, the tonic current was decreased in both the saline ( $n=10$ ;  $5 \pm 5$  pA) and phenobarbital ( $n=9$ ;  $4 \pm 2$  pA) groups when compared to the P14 time point ( $P=0.012$  and  $P<0.0001$ , respectively). ANOVA revealed a significant main effect of age ( $F_{1,63}=31.35$ ,  $P<0.0001$ ), a significant age-by-treatment interaction ( $F_{1,63}=4.6$ ,  $P=0.037$ ), but no main effect of treatment ( $P=0.11$ ).

Pairwise comparisons also revealed a significantly greater tonic current in phenobarbital, as compared to saline groups at P14 ( $P < 0.05$ ). One cell from the saline-treated group was removed from analysis, as it was a statistical outlier (ROUT test). This had no impact on the statistical significance.

During the course of the above experiments at P14, we noted the occasional presence of giant depolarizing events in either current- or voltage-clamp as in the examples shown in Fig. 5A E-F. We analyzed recordings from 22 control cells and 22 cells from phenobarbital treated animals. These events are reminiscent of the giant depolarizing potentials that have been well-described in the developing hippocampus, most notably in the early postnatal period (e.g., during the first postnatal week).<sup>21,26,27</sup>

We calculated the proportion of recorded cells within an animal that displayed GDPs (Figure 5C); the mean percentage of cells with at least one GDP was 25% in saline-treated animals, and 73.3% in phenobarbital treated animals. This reached the level of statistical significance ( $t = 3.714$ ,  $df = 8$ ,  $P < 0.01$ ). GDPs were present in cells from all animals treated with PB, and in four of five animals treated with saline. The proportion of total cells displaying GDPs differed significantly across treatments (Figure 5D-E, Fisher's exact test,  $P < 0.01$ ). As shown in Figure 5E, the amplitude of GDPs did not differ significantly between treated groups (saline:  $24.4 \pm 13.2$  mV; phenobarbital:  $22.3 \pm 8.5$  mV;  $U = 37$ ,  $P > 0.999$ ).

In most cases, only a small number of GDPs were detected per cell. This, coupled with the relatively short duration of recordings ( $< 5$  min) we employed (as analysis of GDPs was not an *a priori* goal of these experiments), precluded a systematic analysis of GDP frequency. In some cases, (e.g., the example shown in Figure 5A), the frequency of GDPs was as high as  $\sim 0.1$  Hz. A representative GDP recorded in current-clamp is shown in Figures 5B GDPs were never observed after Y-tube application of TTX and BMR, consistent with a network driven, GABA-mediated phenotype.

## Discussion

Here we have shown that a single P7 exposure to phenobarbital induces a dysregulation of hippocampal synaptic development. This effect was characterized by increased mIPSCs and GABA-mediated tonic currents in CA1 pyramidal neurons at P14, increased detection of giant depolarizing potentials in animals exposed to phenobarbital at P14, and a failure of phenobarbital exposed animals to show the normal developmental increase in mIPSC frequency between P14 and P29. These data demonstrate that even an acute exposure to PB can produce lasting changes, with consequences of exposure long outlasting the duration of drug action. Thus, the previously reported transient increases in apoptosis caused by PB likely represent only the first signs of damage, with network reorganization and synaptic alterations outlasting the initial exposure and impacting cells that *survive* the initial insult. These changes may provide a link between acute phenobarbital exposure early in life with later-life alterations in cognitive function.

During the course of typical hippocampal development, the input resistance ( $R_m$ ) of CA1 neurons reaches adult-like levels by the end of the second postnatal week.<sup>28</sup> Similarly, the



membrane time constant has been reported to increase by ~25% from P10 to P15.<sup>29</sup> Moreover, increased membrane capacitance (~2x) has been reported in synaptically mature vs. immature CA1 neurons.<sup>27</sup> No differences were found in the saline-treated animals as a function of age (P14 vs. P29+), consistent with the reported time course of maturation for these parameters. Moreover, we found no difference in  $R_m$  between treated groups, but a faster time constant and reduced capacitance in neurons from animals exposed to phenobarbital. These phenotypes may be consistent with a less mature neuronal phenotype in cells from phenobarbital treated animals.

Our finding that phenobarbital exposure increased the frequency of mIPSCs is similar to that seen after neonatal anesthesia exposure. For example, neonatal exposure to propofol results in an increase in mIPSC, but not sIPSC frequency in CA1 neurons.<sup>30,31</sup> A similar profile has been reported after sevoflurane exposure.<sup>32</sup> Interestingly, etomidate exposure during the same period (i.e., P4-P6) does not induce long-term alterations in IPSC frequency.<sup>33</sup> Collectively, these data, along with our current experiments suggest that not all GABA-acting agents produce equivalent profiles of developmental disruption. The case of etomidate is particularly interesting, as the degree to which it induces apoptosis during brain development is unknown. The only study to evaluate etomidate effects on apoptosis was conducted in P10 animals,<sup>34</sup> a sub-optimal time point, as it is beyond the period of typical vulnerability to pro-apoptotic effects of anesthetics and anti-seizure medications. The degree to which the effects we report here with phenobarbital and others have reported with propofol and sevoflurane will generalize to drugs with a non-GABAergic mechanism of action remains to be studied. This is of particular importance as many classes of anti-seizure medications work through alternative pathways. For example, voltage gated sodium channel blockers (e.g., phenytoin, carbamazepine, lamotrigine) all *are capable of* inducing apoptosis; phenytoin does so at therapeutically relevant doses,<sup>5,7</sup> carbamazepine at supratherapeutic doses, and lamotrigine at supratherapeutic doses or as part of polytherapy with other drugs.<sup>35,36</sup> Moreover, phenytoin and lamotrigine both disrupt striatal synaptic maturation.<sup>11</sup> It would thus be of interest to determine if these compounds, like phenobarbital, also impair hippocampal synaptic maturation.

The increase in mIPSC frequency we observed at P14 was reversed by P29+. In saline-exposed animals a normal developmental increase in mIPSC frequency was observed from P14 to P29; this is consistent with the previously reported developmental increases in mIPSC frequency in CA1.<sup>37,38</sup> In contrast to the pattern seen in the saline-exposed group, the phenobarbital-exposed group did not display a developmental increase in mIPSC frequency; by P29, this group displayed a significantly lower frequency than the age-matched saline group. This is similar to the profile we have previously reported in striatum after neonatal phenobarbital exposure. In striatum, a less mature profile of synaptic development was found after exposure to phenobarbital, phenytoin, or lamotrigine. This was reflected by a *decrease* in both IPSC and EPSC frequency.<sup>11</sup> Furthermore, the less mature network phenotype we observed in phenobarbital-exposed slices, which was marked by the persistence of GDPs, is likewise consistent with the less mature network status previously reported in striatum. We found an increase in sIPSC amplitude from P14 to P29+ in saline, but not phenobarbital-treated groups. This increase in sIPSC amplitude is consistent with a

prior report.<sup>38</sup> Similarly consistent with prior reports, we found a speeding of decay kinetics for mIPSCs across the developmental window studied.<sup>37,38</sup>

The hippocampal network implications of heightened early-life mIPSC frequency, followed by impaired later-in-life mIPSC frequency in the present study are unknown. However, the differences in IPSC frequency between groups, which were not accompanied by differences in amplitude or decay kinetics suggests a presynaptic alteration in GABAergic interneurons activity. This finding would be consistent with either a change in release probability or number of synapses. Given the dissociation between the impact of PB exposure on mIPSC and sIPSCs, an interesting avenue for future exploration will be to examine feed-forward inhibition of GABAergic microcircuits within CA1. In the presence of intact network activity, enhanced action potential evoked IPSC frequency may be held in check by a subsequent reduction in the activity of interneurons. Thus, the impact of PB exposure on interneurons within this region will be important to examine.

The increased number of giant depolarizing potentials in phenobarbital exposed animals likewise suggests a less mature hippocampal phenotype. While these large amplitude, GABA-mediated events are best described in the CA3 subfield of the hippocampus,<sup>26</sup> they can be detected throughout all subregions of the hippocampus. These events have been proposed as a mechanism to help synchronize early hippocampal networks and promote synaptic development. In the rat, GDPs occur with a low (0.1Hz) frequency in CA1 between P5 and P7.<sup>39</sup> Indeed, by P12, less than half of slices display GDPs, whereas in the first postnatal week, they are ubiquitous.<sup>40</sup> The early network oscillations in CA1 that are driven by these GDPs occur early in postnatal development and are absent by P15/16.<sup>27</sup> Here, we found that GDPs persisted in slices from animals treated with phenobarbital, albeit with very low occurrence. While rare in recordings from control animals, GDPs were present in 68% of cells from animals treated with phenobarbital. The persistence of these GDPs brings further support to a less mature network phenotype with phenobarbital exposure.

The functional significance of the persistence of these large GABAergic events likely depends on the maturational state of the hippocampus. Early in postnatal development, GABA is excitatory; depolarizing effects of GABA are due to the high intracellular chloride concentration in developing neurons. Typically, by the third postnatal week, neurons in CA1 exhibit adult-like GABA reversal potentials ( $E_{GABA}$ ).<sup>41</sup> For neurons with immature  $E_{GABA}$ , the persistence of large, coordinated GABAergic events would be expected to be excitatory (i.e., a GDP). For neurons with mature  $E_{GABA}$  such coordinated GABAergic input would be profoundly inhibitory. Note that in whole-cell recording, we cannot determine the degree to which the giant potentials we detected would be depolarizing or hyperpolarizing for a given cell at its physiological chloride concentration, but given our findings, changes in  $E_{GABA}$  with phenobarbital treatment should be further investigated.

Tonic GABA currents are present early in development in the hippocampus where they exert a depolarizing influence on pyramidal cells in CA1.<sup>42</sup> In fact, this tonic current appears *prior* to synaptic currents in the developing hippocampus,<sup>43</sup> and may contribute to the excitation needed for early network oscillations.<sup>21</sup> The enhanced tonic current we observed in neurons from phenobarbital exposed rats may thus be consistent with the higher frequency of GDPs

we observed. In hippocampal neurons tonic GABA currents are primarily mediated by alpha5 and delta subunit containing GABA receptors.<sup>44</sup> The degree to which alterations in the expression of these subunits can account for the increased tonic current we observed in PB treated animals, or by contrast, the degree to which changes in network activity leading to increased ambient GABA can account for these findings, remains to be explored. It is worth noting that the enhanced tonic GABA conductance observed in phenobarbital-exposed animals at P14 co-occurred with heightened mIPSC frequency. This effect was not present later in life, where both phenobarbital and control groups displayed significantly less tonic current than early in development. The degree to which increased extrasynaptic GABA is elevated early in life after phenobarbital exposure, perhaps secondarily to increased IPSC frequency, remains to be explored.

Neonatal phenobarbital exposure has been associated with a host of alterations in behavior, including behavioral domains that are linked to hippocampal function. Hippocampal-associated deficits after early life phenobarbital exposure include impaired Morris water maze learning and retention,<sup>14,19</sup> deficits in passive avoidance,<sup>15,16</sup> deficits in fear conditioning,<sup>14</sup> impaired sensorimotor gating,<sup>12-16</sup> impaired spontaneous alternation in the T-Maze,<sup>20</sup> and impaired radial arm maze performance.<sup>18</sup> Similar profiles of water maze deficits have been reported after anesthesia exposure.<sup>10</sup> Interestingly, sevoflurane, propofol,<sup>45</sup> and isoflurane/nitrous oxide/midazolam<sup>10</sup> all also disrupt long-term potentiation in the hippocampus. The impaired LTP reported after anesthesia exposure, along with the alterations in CA1 synaptic development we report here, underscore the importance of future characterization of LTP following early life phenobarbital exposure.

Our present study adds to a growing literature documenting long-lasting impacts of early life exposure to anti-seizure medications. Our findings indicate a less mature network phenotype in the hippocampus of phenobarbital exposed rat pups, and provide a possible mechanism bridging early-life exposure to phenobarbital with the lasting behavioral changes that have reported. Identification of strategies to mitigate these changes in synaptic transmission and/or identification of anti-seizure therapies that avoid these deleterious effects may enable improved treatment of seizures in pregnant women with epilepsy and neonates. Further characterization of the neurophysiological and neurodevelopmental impact of exposure to phenobarbital, and other anti-seizure medications, is clearly warranted.

## Acknowledgments

**Funding sources.** This work was funded by KL2TR001432 to PAF and CONACyT (Mexican Council on Science and Technology) Scholarship #381291 to ASR.

## Abbreviations

<b>PHB</b>	phenobarbital
<b>BMR</b>	bicuculline methobromide
<b>TTX</b>	tetrodotoxin
<b>GDP</b>	giant depolarizing potential

## IPSC                      inhibitory postsynaptic current

### References

1. Glass HC, Kan J, Bonifacio SL, et al. Neonatal seizures: treatment practices among term and preterm infants. *Pediatr Neurol.* 2012;46:111–5. [PubMed: 22264706]
2. Painter MJ, Scher MS, Stein AD, et al. Phenobarbital compared with phenytoin for the treatment of neonatal seizures. *N Engl J Med.* 1999;341:485–9. [PubMed: 10441604]
3. Farwell JR, Lee YJ, Hirtz DG, et al. Phenobarbital for febrile seizures--effects on intelligence and on seizure recurrence. *N Engl J Med.* 1990;322:364–9. [PubMed: 2242106]
4. Dobbing J, Sands J. Comparative aspects of the brain growth spurt. *Early Hum Dev.* 1979;3:79–83. [PubMed: 118862]
5. Bittigau P, Sifringer M, Genz K, et al. Antiepileptic drugs and apoptotic neurodegeneration in the developing brain. *Proc Natl Acad Sci U A.* 2002;99:15089–94.
6. Brown L, Guthertz S, Kulick C, et al. Profile of retigabine-induced neuronal apoptosis in the developing rat brain. *Epilepsia.* 2016;57:660–70. [PubMed: 26865186]
7. Forcelli PA, Kim J, Kondratyev A, et al. Pattern of antiepileptic drug-induced cell death in limbic regions of the neonatal rat brain. *Epilepsia.* 2011;52:e207–211. [PubMed: 22050285]
8. Kaushal S, Tamer Z, Opoku F, et al. Anticonvulsant drug-induced cell death in the developing white matter of the rodent brain. *Epilepsia.* 2016;57:727–34. [PubMed: 27012547]
9. Ikonomidou C, Bittigau P, Ishimaru MJ, et al. Ethanol-induced apoptotic neurodegeneration and fetal alcohol syndrome. *Science.* 2000;287:1056–60. [PubMed: 10669420]
10. Jevtovic-Todorovic V, Hartman RE, Izumi Y, et al. Early exposure to common anesthetic agents causes widespread neurodegeneration in the developing rat brain and persistent learning deficits. *J Neurosci Off J Soc Neurosci.* 2003;23:876–82.
11. Forcelli PA, Janssen MJ, Vicini S, et al. Neonatal exposure to antiepileptic drugs disrupts striatal synaptic development. *Ann Neurol.* 2012;72:363–72. [PubMed: 22581672]
12. Forcelli PA, Janssen MJ, Stamps LA, et al. Therapeutic strategies to avoid long-term adverse outcomes of neonatal antiepileptic drug exposure. *Epilepsia.* 2010;51 Suppl 3:18–23.
13. Bhardwaj SK, Forcelli PA, Palchik G, et al. Neonatal exposure to phenobarbital potentiates schizophrenia-like behavioral outcomes in the rat. *Neuropharmacology.* 2012;62:2337–45. [PubMed: 22366076]
14. Forcelli PA, Kozlowski R, Snyder C, et al. Effects of neonatal antiepileptic drug exposure on cognitive, emotional, and motor function in adult rats. *J Pharmacol Exp Ther.* 2012;340:558–66. [PubMed: 22129597]
15. Frankel S, Medvedeva N, Guthertz S, et al. Comparison of the long-term behavioral effects of neonatal exposure to retigabine or phenobarbital in rats. *Epilepsy Behav EB.* 2016;57:34–40.
16. Guthertz SB, Kulick CV, Soper C, et al. Brief postnatal exposure to phenobarbital impairs passive avoidance learning and sensorimotor gating in rats. *Epilepsy Behav EB.* 2014;37:265–9.
17. Mikulecká A, Subrt M, Stuchlík A, et al. Consequences of early postnatal benzodiazepines exposure in rats. I. Cognitive-like behavior. *Front Behav Neurosci.* 2014;8:101. [PubMed: 24734010]
18. Pick C, Yanai J. Long term reduction in eight arm maze performance after early exposure to phenobarbital. *Int J Dev Neurosci.* 1985;3:223–7. [PubMed: 24874750]
19. Stefovská VG, Uckermann O, Czuczwar M, et al. Sedative and anticonvulsant drugs suppress postnatal neurogenesis. *Ann Neurol.* 2008;64:434–45. [PubMed: 18991352]
20. Pick C, Yanai J. Long-term reduction in spontaneous alternations after early exposure to phenobarbital. *Int J Dev Neurosci.* 1984;2:223–8. [PubMed: 24874036]
21. Cellot G, Cherubini E. Functional role of ambient GABA in refining neuronal circuits early in postnatal development. *Front Neural Circuits.* 2013;7:136. [PubMed: 23964205]
22. Kubova H, Mares P. Anticonvulsant effects of phenobarbital and primidone during ontogenesis in rats. *Epilepsy Res.* 1991;10:148–55. [PubMed: 1817955]

23. Forcelli PA, Soper C, Duckles A, et al. Melatonin potentiates the anticonvulsant action of phenobarbital in neonatal rats. *Epilepsy Res.* 2013;107:217–23. [PubMed: 24206906]
24. Ting JT, Daigle TL, Chen Q, et al. Acute brain slice methods for adult and aging animals: application of targeted patch clamp analysis and optogenetics. *Methods Mol Biol Clifton NJ.* 2014;1183:221–42.
25. Vicini S, Ferguson C, Prybylowski K, et al. GABA(A) receptor alpha1 subunit deletion prevents developmental changes of inhibitory synaptic currents in cerebellar neurons. *J Neurosci.* 2001;21:3009–16. [PubMed: 11312285]
26. Ben-Ari Y, Cherubini E, Corradetti R, et al. Giant synaptic potentials in immature rat CA3 hippocampal neurones. *J Physiol.* 1989;416:303–25. [PubMed: 2575165]
27. Tyzio R, Represa A, Jorquera I, et al. The establishment of GABAergic and glutamatergic synapses on CA1 pyramidal neurons is sequential and correlates with the development of the apical dendrite. *J Neurosci Off J Soc Neurosci.* 1999;19:10372–82.
28. Spigelman I, Zhang L, Carlen PL. Patch-clamp study of postnatal development of CA1 neurons in rat hippocampal slices: membrane excitability and K<sup>+</sup> currents. *J Neurophysiol.* 1992;68:55–69. [PubMed: 1517828]
29. Baraban SC, McCarthy EB, Schwartzkroin PA. Evidence for increased seizure susceptibility in rats exposed to cocaine in utero. *Dev Brain Res.* 1997;102:189–96. [PubMed: 9352101]
30. Xu C, Seubert CN, Gravenstein N, et al. Propofol, but not etomidate, increases corticosterone levels and induces long-term alteration in hippocampal synaptic activity in neonatal rats. *Neurosci Lett.* 2016;618:1–5. [PubMed: 26923669]
31. Tan S, Xu C, Zhu W, et al. Endocrine and Neurobehavioral Abnormalities Induced by Propofol Administered to Neonatal Rats: *Anesthesiology.* 2014;121:1010–7. [PubMed: 24992523]
32. Xu C, Tan S, Zhang J, et al. Anesthesia with sevoflurane in neonatal rats: Developmental neuroendocrine abnormalities and alleviating effects of the corticosteroid and Cl(–) importer antagonists. *Psychoneuroendocrinology.* 2015;60:173–81. [PubMed: 26150359]
33. Zhang J-Q, Xu W-Y, Xu C-Q. Neonatal Propofol and Etomidate Exposure Enhance Inhibitory Synaptic Transmission in Hippocampal Cornu Ammonis 1 Pyramidal Neurons. *Chin Med J (Engl).* 2016;129:2714–24. [PubMed: 27824005]
34. Nyman Y, Fredriksson A, Lönnqvist P-A, et al. Etomidate exposure in early infant mice (P10) does not induce apoptosis or affect behaviour. *Acta Anaesthesiol Scand.* 2016;60:588–96. [PubMed: 26763687]
35. Katz I, Kim J, Gale K, et al. Effects of lamotrigine alone and in combination with MK-801, phenobarbital, or phenytoin on cell death in the neonatal rat brain. *J Pharmacol Exp Ther.* 2007;322:494–500. [PubMed: 17483293]
36. Kim J, Kondratyev A, Gale K. Antiepileptic drug-induced neuronal cell death in the immature brain: effects of carbamazepine, topiramate, and levetiracetam as monotherapy versus polytherapy. *J Pharmacol Exp Ther.* 2007;323:165–73. [PubMed: 17636003]
37. Cohen AS, Lin DD, Coulter DA. Protracted postnatal development of inhibitory synaptic transmission in rat hippocampal area CA1 neurons. *J Neurophysiol.* 2000;84:2465–76. [PubMed: 11067989]
38. Banks MI, Hardie JB, Pearce RA. Development of GABA(A) receptor-mediated inhibitory postsynaptic currents in hippocampus. *J Neurophysiol.* 2002;88:3097–107. [PubMed: 12466433]
39. Wester JC, McBain CJ. Interneurons Differentially Contribute to Spontaneous Network Activity in the Developing Hippocampus Dependent on Their Embryonic Lineage. *J Neurosci Off J Soc Neurosci.* 2016;36:2646–62.
40. Khazipov R, Khalilov I, Tyzio R, et al. Developmental changes in GABAergic actions and seizure susceptibility in the rat hippocampus. *Eur J Neurosci.* 2004;19:590–600. [PubMed: 14984409]
41. Zhang L, Spigelman I, Carlen PL. Development of GABA-mediated, chloride-dependent inhibition in CA1 pyramidal neurones of immature rat hippocampal slices. *J Physiol.* 1991;444:25–49. [PubMed: 1822551]
42. Marchionni I, Omrani A, Cherubini E. In the developing rat hippocampus a tonic GABA<sub>A</sub>-mediated conductance selectively enhances the glutamatergic drive of principal cells: GABA<sub>A</sub>-

- mediated conductance in the developing hippocampus. *J Physiol.* 2007;581:515–28. [PubMed: 17317750]
43. Demarque M, Represa A, Becq H, et al. Paracrine intercellular communication by a Ca<sup>2+</sup>- and SNARE-independent release of GABA and glutamate prior to synapse formation. *Neuron.* 2002;36:1051–61. [PubMed: 12495621]
  44. Scimemi A, Semyanov A, Sperk G, et al. Multiple and plastic receptors mediate tonic GABA<sub>A</sub> receptor currents in the hippocampus. *J Neurosci Off J Soc Neurosci.* 2005;25:10016–24.
  45. Gao J, Peng S, Xiang S, et al. Repeated exposure to propofol impairs spatial learning, inhibits LTP and reduces CaMKII $\alpha$  in young rats. *Neurosci Lett.* 2014;560:62–6. [PubMed: 24333173]

**Significance:**

These neurophysiological alterations following phenobarbital exposure provide a potential mechanism by which acute phenobarbital exposure can have a long-lasting impact on brain development and behavior.

**Key Points**

Phenobarbital (PB) is widely utilized for the treatment of neonatal seizures

Early life PB exposure causes lasting changes in brain development and behavior

Early life PB disrupted inhibitory synaptic development in CA1 neurons

Early life PB increased later-in-life giant depolarizing potential occurrence in CA1

Author Manuscript

Author Manuscript

Author Manuscript

Author Manuscript



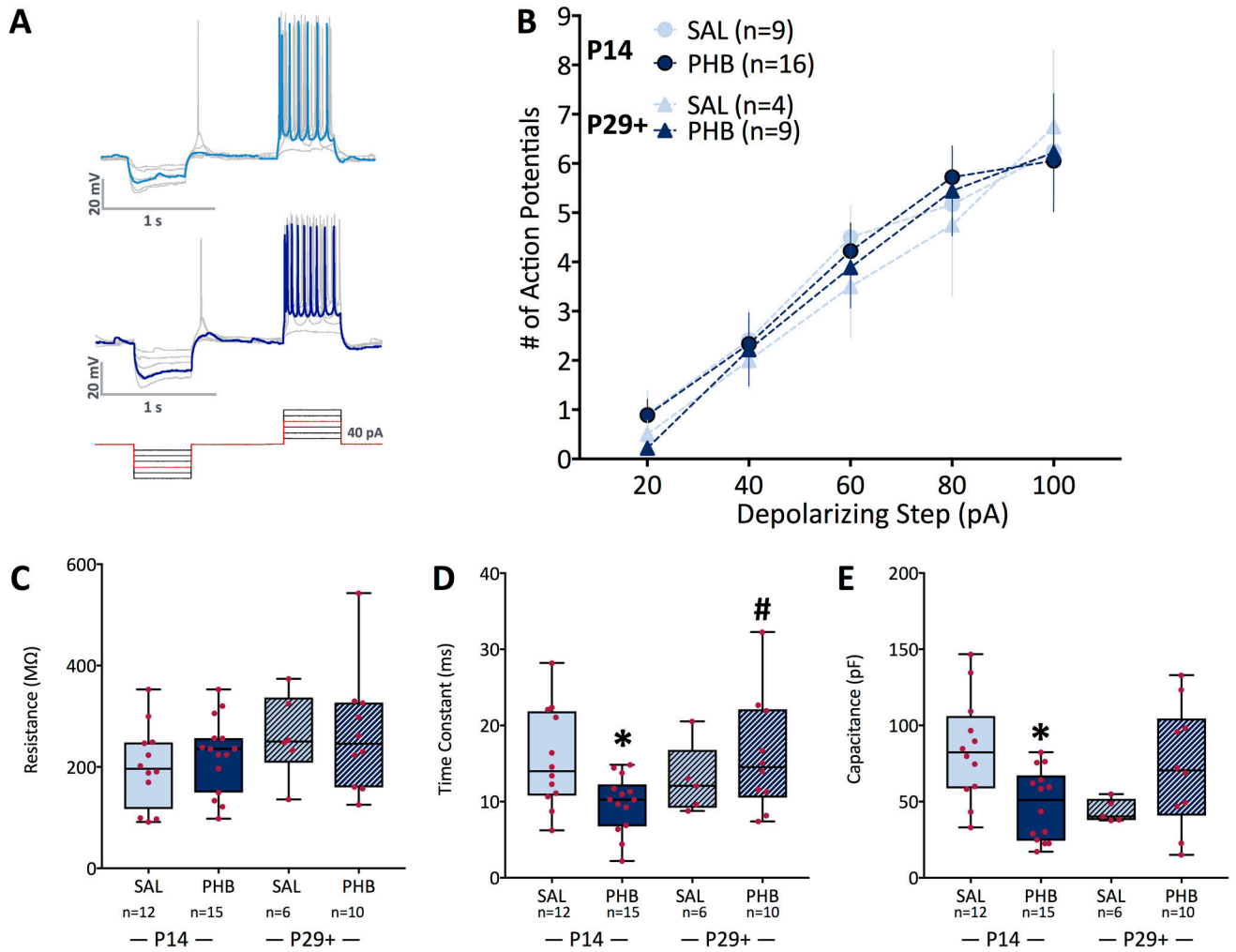


**Figure 1. Properties of CA1 neurons recorded from phenobarbital and saline-treated pups.** (A) Representative traces showing action potentials fired by CA1 neurons to depolarizing current steps in current-clamp configuration. Mean number of action potentials in CA1 neurons in response to depolarizing current steps are quantified in (B), from the P14 time point. (C) Input resistance, individual cell values are overlaid on the box and whisker plots. (D) Membrane time constant \* = significantly different than saline,  $P < 0.05$ ; # = significantly different P14 to P29+,  $P < 0.05$ . (E) Membrane capacitance \* = significantly different than saline at P14,  $P < 0.05$ .

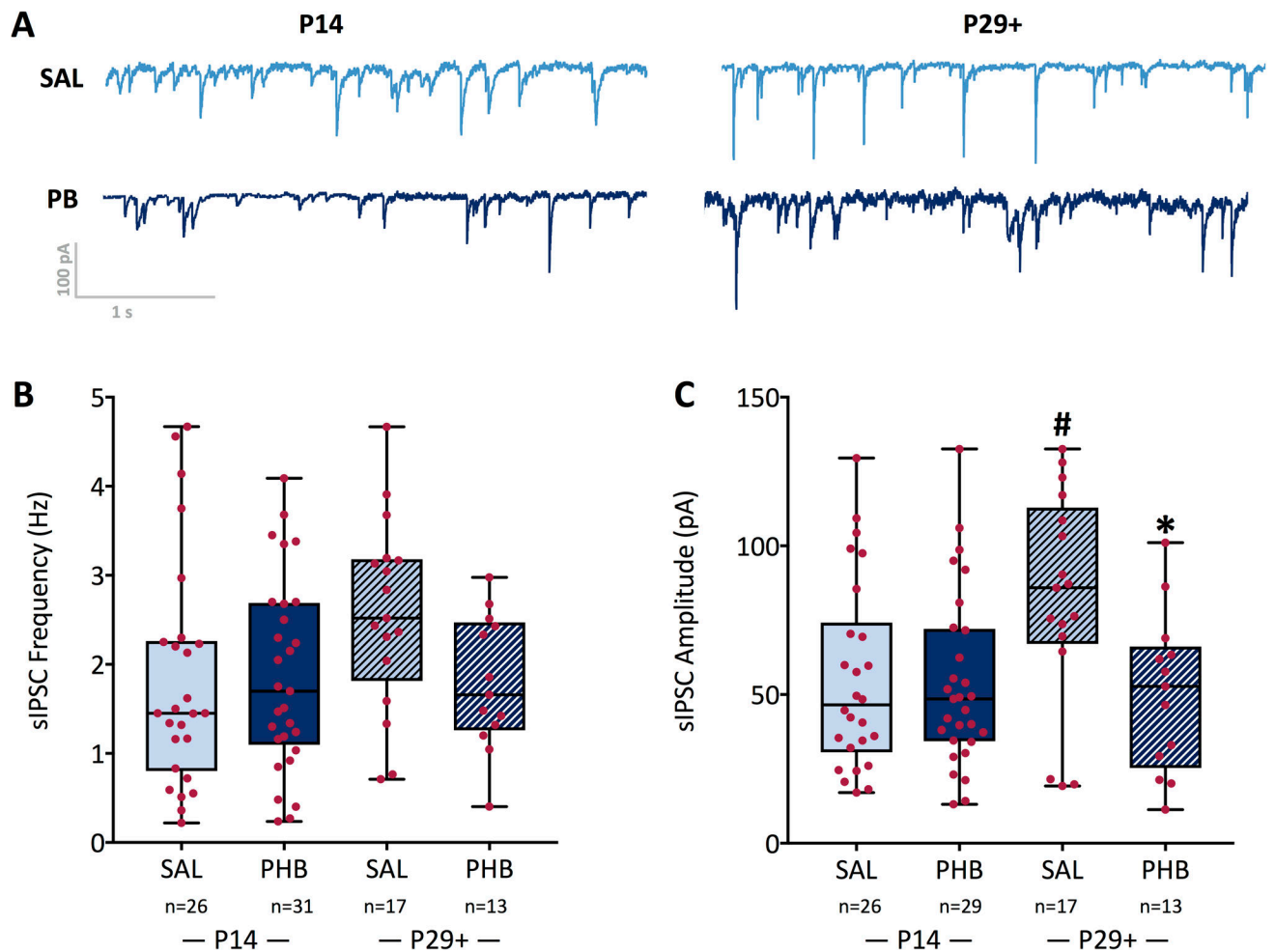


**Figure 2. Spontaneous IPSCs are unaltered by developmental exposure to phenobarbital.**

(A) Representative sIPSCs from cells from a saline and a phenobarbital treated animal at each age (B) sIPSC frequency and (C) amplitude did not differ between treatment groups at P14. From P14 to P29+, a developmental increase in sIPSC amplitude was evident in the saline exposed group, but not in the phenobarbital exposed group. This resulted in a significantly smaller sIPSC amplitude in phenobarbital, as compared to saline-exposed animals at P29+ ( $P < 0.05$ ). \* = significantly different than saline within age group,  $P < 0.05$ ; # = significantly difference between P14 and P29+ for a given drug treatment,  $P < 0.05$ .

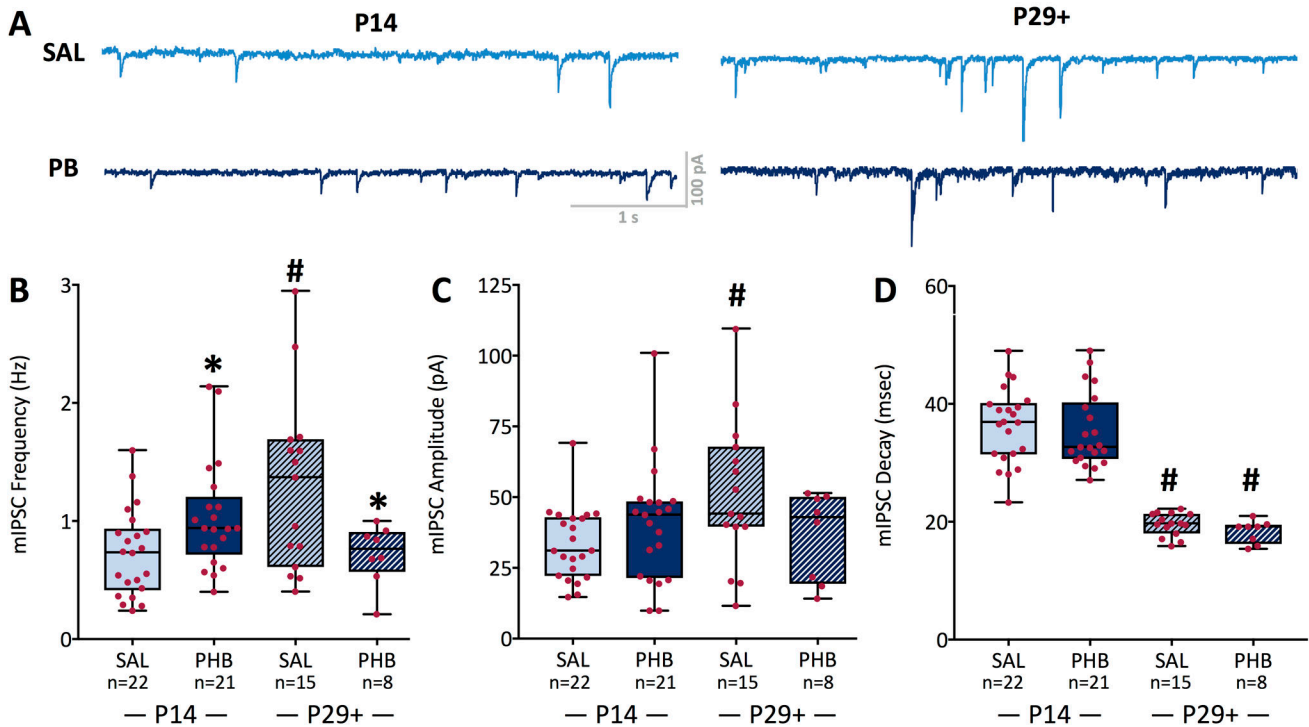


**Figure 3. The developmental maturation of miniature IPSC frequency is disrupted following early-life exposure to phenobarbital.**

(A) Representative mIPSCs in CA1 pyramidal neurons at different ages and treatments. (B) Frequency of mIPSC was increased in the phenobarbital exposed group at P14 ( $P < 0.05$ ). From P14 to P29+ there was a significant increase in mIPSC frequency in the saline group ( $P < 0.05$ ). The phenobarbital exposed group did not display the expected developmental increase in mIPSC frequency between P14 and P29+, and the mIPSC frequency in this group was thus significantly less than that in the saline group at P29+ ( $P < 0.05$ ). Neither mIPSC amplitude (C) nor decay (D) differed between treatment groups. However, mIPSC amplitude was significantly greater in the saline-exposed at P29+ compared to P14 ( $P < 0.05$ ). Moreover, mIPSC decay was significantly faster in both the saline and phenobarbital groups at P29+ as compared to P14 ( $P < 0.05$ ). \* = significantly different than saline within age group,  $P < 0.05$ ; # significantly difference between P14 and P29+ for a given drug treatment,  $P < 0.05$ .

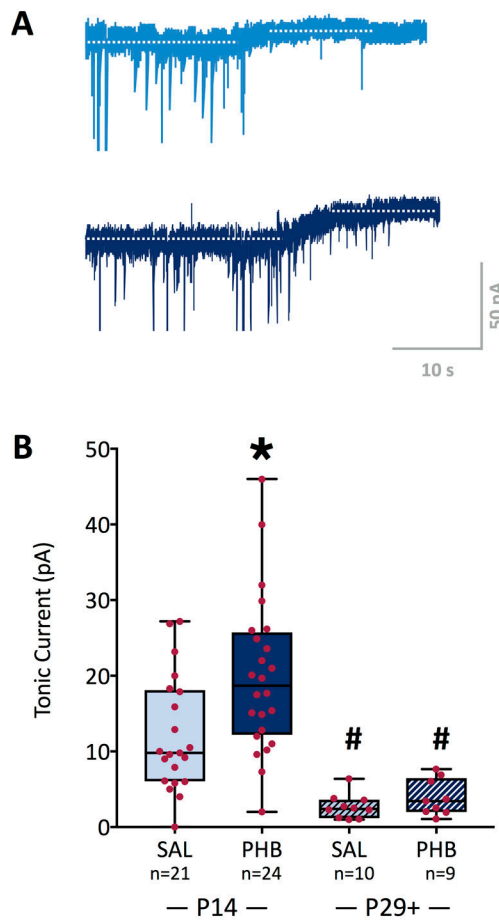


**Figure 4. Developmental exposure to phenobarbital increases tonic GABA current.**

A) Representative recordings (at P14) showing the shift in holding current after the application of bicuculline methobromide (BMR) indicating the presence of a tonic GABA current. (B) Tonic GABA current was significantly increased as compared to saline at P14; at P29+, tonic current did not differ between treatments, and was significantly ( $P < 0.05$ ) reduced compared to P14. (\* = significantly different than saline within age group,  $P < 0.05$ ; # significantly difference between P14 and P29+ for a given drug treatment,  $P < 0.05$ ).

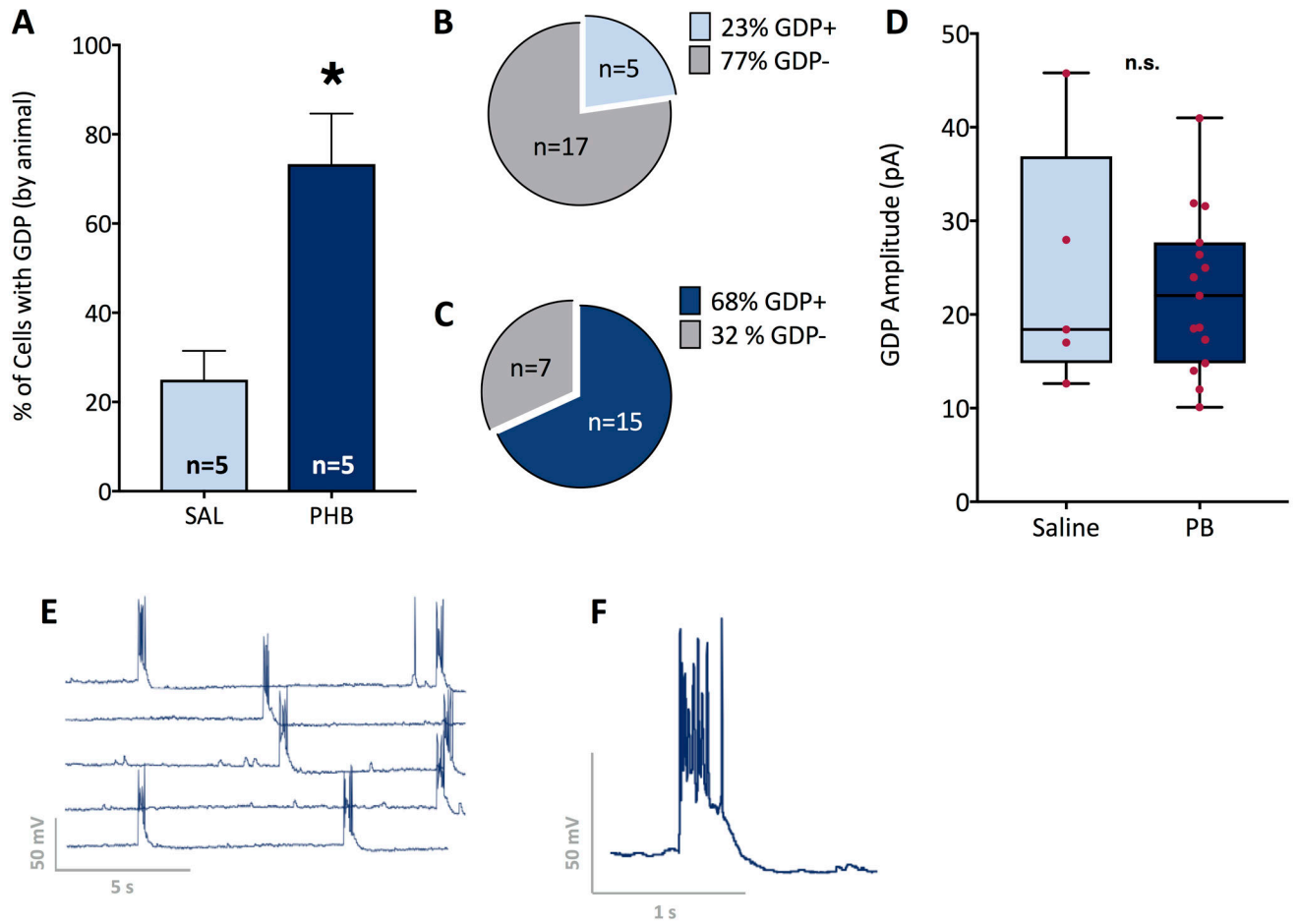


**Figure 5. Developmental exposure to phenobarbital results in increased occurrence of giant depolarizing potentials.**

(A) Representative current clamp trace recorded from a neuron in the phenobarbital exposed group; the frequency of GDP occurrence in this cell was ~0.1 Hz. (B) Expanded view of a GDP from (E). (C) GDP frequency tabulated on an animal-by-animal basis; \* = significantly different than saline,  $P < 0.05$ . (D, E) GDP frequency tabulated as a function of total cells recorded from the saline (D) and phenobarbital (E) treated groups. (E) GDP amplitude did not differ between groups n.s. = not significantly different.